Epoxy Composite Fibers Reinforced with Aligned Single-Walled Carbon Nanotubes Functionalized with Generation 0−2 Dendritic Poly(amidoamine)

Jianfei Che,[†] Wei Yuan,[†] Guohua Jiang,[†] Jie Dai,[‡] Su Yin Lim,[§] and Mary B. Chan-Park*,[†]

*School of Chemical and Biomedical Engineering, Nanyang Technological University,
62 Nanyang Drive, Singapore 637459, Singapore, DSO National Laboratories, 20 Science Park Drive,
Singapore 118230, Singapore, and Directorate of Research and Development, Defence Science &
Technology Agency, 71 Science Park Drive, Singapore 118253, Singapore*

Single-walled carbon nanotubes functionalized with generation (n) 0−2 dendritic poly(amidoamine) (denoted as SWNTs-G$_n$-NH$_2$, n = 0, 1, or 2) were used as filler in thermosetting epoxy to prepare anisotropic microscale diameter fibers by reactive spinning. Dendritic poly(amidoamine) (PAMAM) was "grafted from" acid-modified and toluene 2,4-diisocyanate-activated SWNTs by repeating amidation of terminal ester groups via ethylenediamine (EDA) and Michael addition of methyl acrylate (MA) to amino groups. Fourier transform infrared (FTIR) and hydrogen nuclear magnetic resonance (^{1}H NMR) spectroscopy and thermogravimetric analysis (TGA) confirmed the successful grafting and generation buildup. Optical and scanning electron microscope (SEM) observations revealed that PAMAM-functionalized SWNTs dispersed in epoxy much more uniformly than pristine nanotubes. The dispersibility improved with increasing generation number. Microsized fibers made of epoxy reinforced with aligned SWNTs-G$_2$-NH$_2$ by reactive spinning show high tensile strength and Young's modulus per unit weight fraction (dσ/dW_{NT} and dE/dW_{NT}). The respective measures are 7022 MPa and 118.0 GPa, which is a high reinforcement efficacy in comparison to other fillers. The nanotube alignment and grafting of dendritic PAMAM play a crucial role in the enhancement of the tensile strength of these reinforced composite fibers.

Introduction

The synthesis of carbon nanotube (CNT) nanocomposites with enhanced mechanical properties requires precise control of the microstructure of the composites. To achieve effective reinforcement, the filler must fulfill four main requirements: high aspect ratio, homogeneous dispersion, efficient interfacial stress transfer, and good alignment.[1,2] Simultaneous fulfillment of all of these has not been trivial. In thermoplastics, the high viscosity enables the CNTs to be better dispersed by techniques such as shear mixing and elongational flow mixing.[3] Thus far, the improvements in tensile properties achieved in thermosetting epoxy composites have been poor compared to those in thermoplastics composites (Table 1).

Table 1. Summary and Comparison of Reinforcement of SWNT Epoxy Composite*

	dσ/dW_{NT} (MPa)		dE/dW_{NT} (GPa)	
	mean	max	mean	max
2003[4]	1180	1180	60.6	60.6
2004[5]	2100	2100	62.4	62.4
2005[6]	1160	1160	71.0	71.0
2006[7]	3600	3600	35.0	35.0
2008[3,8,9]	742	1060	346.5	620.0
our results	7022		118.0	

* dσ/dW_{NT} and dE/dW_{NT}: the variation rate of tensile strength and Young's moduli with weight fraction, respectively.

Carbon nanotubes that have not been excessively chopped possess high aspect ratio. A reactive surfactant that can disperse CNTs homogeneously in the polymer matrix and also form covalent bonding between the nanotubes and polymer matrix can effectively transfer mechanical load.[10−13] Dendrimers are attractive as surfactants and CNT debundling additives, as they are known to be highly effective steric stabilizers (Scheme 1).[14−18] Some studies have reported synthetic methods to functionalize CNTs with dendritic

* Corresponding author. E-mail: mbechan@ntu.edu.sg.
† Nanyang Technological University.
‡ DSO National Laboratories.
§ Defence Science & Technology Agency.
(1) Coleman, J. N.; Khan, U. Y.; Gun'ko, K. *Adv. Mater.* **2006,** *18,* 689.
(2) Moniruzzaman, M.; Winey, K. I. *Macromolecules* **2006**, *39,* 5194.
(3) Sun, L.; Warren, G. L.; O'Reilly, J. Y.; Everett, W. N.; Lee, S. M.; Davis, D.; Lagoudas, D.; Sue, H.-J. *Carbon* **2008**, *46,* 320.
(4) Zhu, J.; Kim, J. D.; Peng, H. Q.; Margrave, J. L.; Khabashesku, V. N.; Barrera, E. V. *Nano Lett.* **2003**, *3,* 1107.
(5) Zhu, J.; Peng, H. Q.; Rodriguez-Macias, F.; et al. *Adv. Funct. Mater.* **2004**, *14,* 643.
(6) Gojny, F. H.; Wichmann, M. H. G.; Fiedle, B. *Compos. Sci. Technol.* **2005**, *65,* 2300.
(7) de Villoria, R. G.; Miravete, A.; Cuartero, J.; et al. *Compos. Part B* **2006**, *37,* 273.

(8) Valentini, L.; Puglia, D.; Carniato, F.; Boccaleri, E.; Marchese, L.; Kenny, J. M. *Compos. Sci. Technol.* **2008**, *68,* 1008.
(9) Li, X. F.; Lau, K. T.; Yin, Y. S. *Compos. Sci. Technol.* **2008**, *68,* 2876.
(10) Graff, R. A.; Swanson, J. P.; Barone, P. W. *Adv. Mater.* **2005**, *17,* 980.
(11) Banerjee, S.; Hemraj-Benny, T.; Wong, S. S. *Adv. Mater.* **2005**, *17,* 17.
(12) Shen, K.; Curran, S.; Xu, H. F. *J. Phys. Chem. B* **2005**, *109,* 4455.
(13) Lau, K. T.; Lu, M.; Lam, C. K. *Compos. Sci. Technol.* **2005**, *65,* 719.

Scheme 1. Schematic of Dispersion of SWNTs Grafted with Dendritic PAMAM
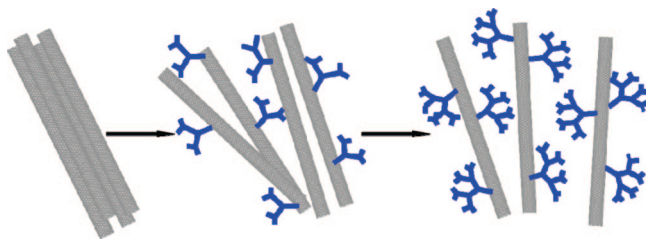
poly(amidoamine) (PAMAM). PAMAM has low melting viscosity, high solubility, and reactive peripheral amine groups that can easily be tailored to control its matrix compatibility and reactions in order to reduce CNT agglomeration and increase interfacial strength.[3,16−18] Sun et al. used preformed generation-0 PAMAM as a reactive surfactant in the fabrication of single-walled carbon nanotubes (SWNT; 1 wt %, randomly oriented in the matrix)/epoxy composites; this improved the modulus and strength by 27% and 12%, respectively.[3]

Grafting of polymers to nanotubes has been realized via both "grafting-to"[19−22] and "grafting-from"[23−26] approaches. The grafting-to method is based on attachment of premade end-functionalized polymer onto the tips and convex walls of the nanotubes via chemical reactions such as etherification and amidization. One advantage of this method is that the mass and distribution of the grafted polymers can be more precisely controlled. However, initial grafted polymer chains sterically prevent diffusion of additional polymer chains to the nanotube surface resulting in low grafting density. The grafting-from method is based on immobilization of reactive groups (initiators) onto the surface, followed by in situ polymerization of appropriate monomers to form polymer-grafted nanotubes. The advantage of this approach is that very high grafting density can be achieved. But careful control of the amount of initiator and the conditions for the polymerization reaction is required.

Rather than the grafting-to method used by Sun et al.,[3] we investigated the grafting-from approach, which involves the propagation of dendrimers from CNT surfaces by in situ polymerization of monomers in the presence of CNT-attached macroinitiators. The mobility and small size of the fugitive monomers, in contrast to that of preformed dendritic polymers, are expected to improve the efficiency and yield of the grafting-from approach and the resulting debundling process. Dendritic PAMAM occupies increasing space as the branch propagates from the central initiating core. The number of peripheral reactive groups can be precisely controlled by choosing the appropriate synthetic generation. Functionalization of nanotubes with dendrimers represents a particularly promising strategy to attach an in-principle unlimited number of functional groups onto the SWNT surfaces, and thus to significantly increase the compatibility and reactivity of CNTs with thermosetting polymer matrices, such as epoxy, bismaleimide, and cyanate ester.

Finally, to achieve good alignment of nanotubes to exploit their superior anisotropic mechanical properties,[1,27] we applied the reactive spinning process previously reported by us.[28] Spinning has been widely used for thermoplastic resins such as polyvinyl acetate (PVA),[29,30] polyamide (PA),[31−33] and polycarbonate (PC),[34,35] but it has rarely been applied to thermosetting resins, except for cyanate ester.[28] Control of viscosity within a narrow range suitable for spinning is often tricky and resin-specific. By comparison with cyanate ester, thermosetting epoxy generally has a smaller range of spinning conditions due to its higher reactivity. However, use of thermoset resins as the matrix for fiber spinning offers advantages of lower viscosity and reaction with functional groups on the nanotubes.

In this paper, we report the grafting-from approach to synthesis of dendritic PAMAM on SWNTs and demonstrate the improved dispersion and high reinforcement efficacy of these functionalized CNTs in an epoxy matrix. Dendrimer-functionalized SWNTs at successive grafting generations (n) from 0 to 2 (SWNT-G_n-NH_2) were synthesized. Fourier transform infrared (FTIR) and hydrogen nuclear magnetic resonance (^{1}H NMR) spectra and thermogravimetric analysis (TGA) confirmed the successful grafting and generation buildup. Reinforced microsized epoxy composite fibers were fabricated by reactive spinning. Fibers were produced from neat epoxy resin and from epoxy reinforced (0.5 wt %) with pristine SWNTs (hereafter labeled as SWNTs-p) or SWNTs functionalized with various generations (0−2) of grafted dendrimers. The fibers were characterized by optical and electron microscopy and tensile tests. The dendritic PAMAM-functionalized SWNTs were uniformly dispersed into the

(14) Tao, L.; Chen, G.; Mantovani, G.; York, S.; Haddleton, D. M. *Chem. Commun.* **2006**, 4949.
(15) Choi, J. Y.; Oh, S. J.; Lee, H. J.; Wang, D. H.; Tan, L. S.; Baek, J. B. *Macromolecules* **2007**, *40*, 4474.
(16) Zeng, Y. L.; Huang, Y. F.; Jiang, J. H.; et al. *Electrochem. Commun.* **2007**, *9*, 185.
(17) Pan, B. F.; Cui, D. X.; Gao, F.; et al. *Nanotechnology* **2006**, *17*, 2483.
(18) Campidelli, S.; Sooambar, C.; Diz, E. L.; et al. *J. Am. Chem. Soc.* **2006**, *128*, 12544.
(19) Gao, J. B.; Itkis, M. E.; Yu, A. P.; Bekyarova, E.; Zhao, B.; Haddon, R. C. *J. Am. Chem. Soc.* **2005**, *127*, 3847.
(20) Qu, L. W.; Lin, Y.; Hill, D. E.; Zhou, B.; Wang, W.; Sun, X. F.; Kitaygorodskiy, A.; Suarez, M.; Connell, J. W.; Allard, L. F.; Sun, Y. P. *Macromolecules* **2004**, *37*, 6055.
(21) Hill, D.; Lin, Y.; Qu, L. W.; Kitaygorodskiy, A.; Connell, J. W.; Allard, L. F.; Sun, Y. P. *Macromolecules* **2005**, *38*, 7670.
(22) Yang, B. X.; Shi, J. H.; Pramoda, K. P.; Goh, S. H. *Nanotechnology* **2007**, *18*, 125606.
(23) Kong, H.; Gao, C.; Yan, D. Y. *Macromolecules* **2004**, *37*, 4022.
(24) Yoon, K. R.; Kim, W. J.; Choi, I. S. *Macromol. Chem. Phys.* **2004**, *205*, 1218.
(25) Viswanathan, G.; Chakrapani, N.; Yang, H. C.; Wei, B. Q.; Chung, H. S.; Cho, K. W.; Ryu, C. Y.; Ajayan, P. M. *J. Am. Chem. Soc.* **2003**, *125*, 9258.
(26) Shanmugharaj, A. M.; Bae, J. H.; Nayak, R. R.; Ryu, S. H. *J. Polym. Sci. Part A Polym. Chem.* **2007**, *45*, 460.
(27) McIntosh, D.; Khabashesku, V. N.; Barrera, E. V. *Chem. Mater.* **2006**, *18*, 4561.
(28) Che, J. F.; Chan-Park, M. B. *Adv. Funct. Mater.* **2008**, *18*, 888.
(29) Vigolo, B.; Penicaud, A.; Coulon, C.; Sauder, C.; Pailler, R.; Journet, C.; Bernier, P.; Poulin, P. *Science* **2000**, *290*, 1331.
(30) Miaudet, P.; Badaire, S.; Maugey, M.; Derre, A.; Pichot, V.; Launois, P.; Poulin, P.; Zakri, C. *Nano Lett.* **2005**, *5*, 2212.
(31) Gao, J. B; Itkis, M. E; Yu, A. P. *J. Am. Chem. Soc.* **2005**, *127*, 3847.
(32) Sandler, J. K. W.; Pegel, S; Cadek, M. *Polymer* **2004**, *45*, 2001.
(33) Jose, M. V.; Steinert, B. W.; Thomas, V.; Dean, D. R.; Abdalla, M. A.; Price, G. M. *Polymer* **2007**, *48*, 1096.
(34) Fornes, T. D; Baur, J. W.; Sabba, Y; Thomas, E. L. *Polymer* **2006**, *47*, 1704.
(35) Potschke, P; Brunig, H; Janke, A; Fischer, D; Jehnichen, D. *Polymer* **2005**, *46*, 10355.

Scheme 2. Grafting of Dendritic PAMAM from SWNT Surface[a]
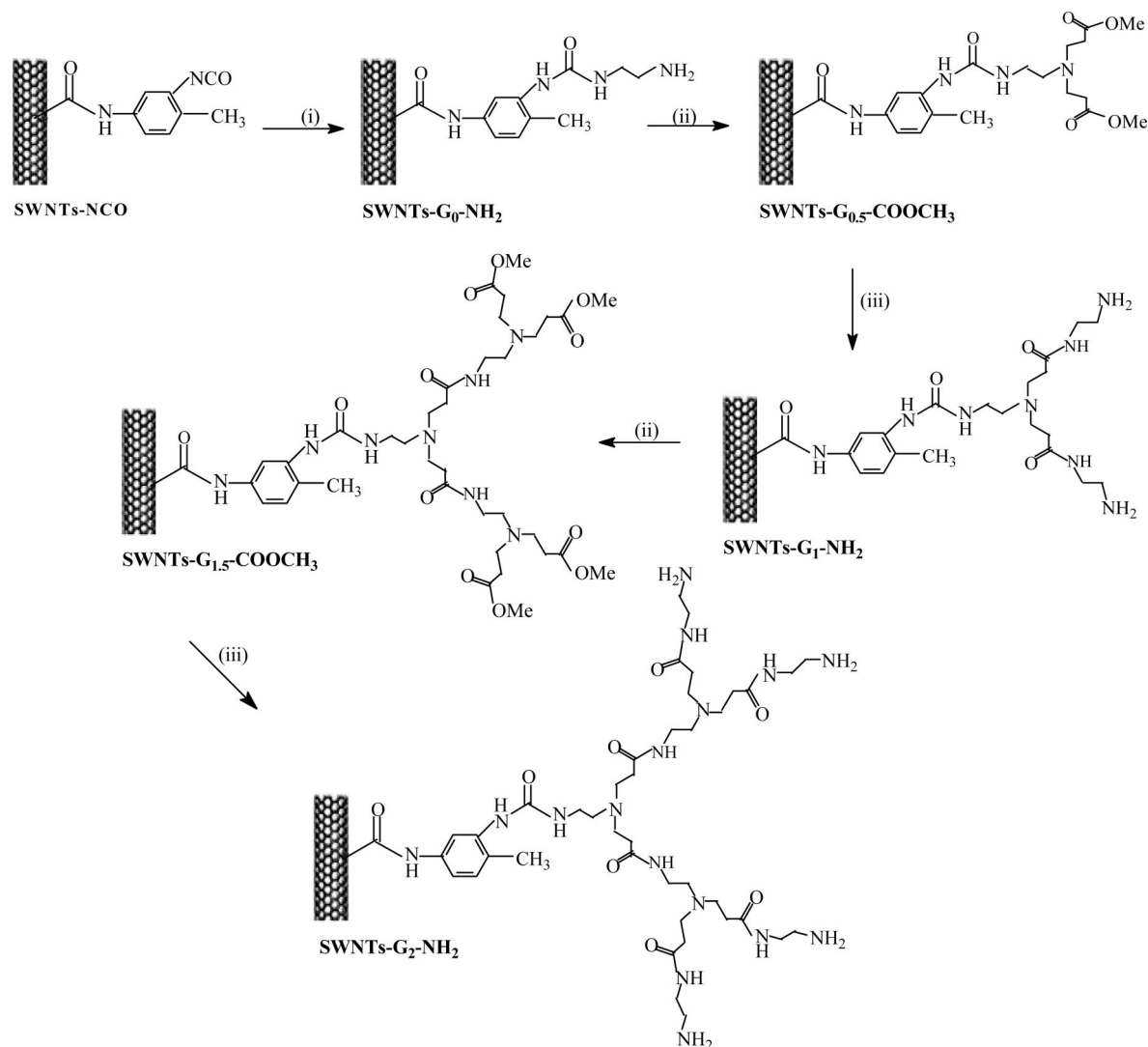
[a] Reagents and conditions: (i) EDA, 60 °C, 24 h; (ii) MA, 30 °C, 48 h; (iii) EDA, 30 °C, 48 h.

epoxy matrix and covalently reacted with the matrix. SWNTs were aligned along the fiber axis in the process of reactive spinning; this alignment plays a crucial role in the enhancement of the tensile strength and modulus of the resulting composite fibers.

Experimental Section

Materials. SWNTs with purity greater than 95% were purchased from Chengdu Research Institute of Organic Chemistry (China). The SWNTs, produced by catalytic chemical vapor deposition, had diameters of about 1–2 nm and lengths of about 5–15 μm. Epoxy matrix was supplied in two parts: Rutapox L20 resin and Rutapox SL hardener, provided by Bakelite AG. Ethylenediamine (EDA), methyl acrylate (MA), and toluene 2,4-diisocyanate (TDI) were obtained from Aldrich. Sulfuric acid (H_2SO_4, 98%), nitric acid (HNO_3, 68%), and other solvents were of analytical grade and used as received.

Preparation of Dendrimer-Functionalized SWNTs. The grafting of dendrimer from SWNT surfaces was achieved via bridging isocyanate, as shown in Scheme 2.

A mild acid treatment of the CNTs was employed in order to avoid severe damage and maintain appropriate lengths with fewer

surface defects. SWNTs-p were purified by thermal treatment at 350 °C for 2 h in air followed by acid oxidation in a mixture of concentrated H_2SO_4 and HNO_3 (3:1) at 60 °C for 3 h to produce carboxyl-functionalized SWNTs. In a final step, the SWNTs were refluxed in 0.5 M HCl for 4 h to ensure conversion of carbonyl terminal groups (which were not sufficiently oxidized by mixed acid) into carboxyl groups, resulting in carboxylic acid-functionalized SWNTs (SWNTs-COOH).

The SWNTs-COOH were then reacted with TDI, a reagent that has been used as a bridging agent for grafting due to its high reactivity.[36] Typically, 0.5 g of SWNTs-COOH was dispersed in 20 mL of anhydrous acetone under sonication at room temperature for 30 min and then an excess of TDI (about 10 mL) was added. The suspension was sonicated in an ice bath for 1 h. Then the amidation reaction was undertaken in a dry nitrogen atmosphere at 50 °C for 24 h. The functionalized SWNT (SWNTs-NCO) suspension was filtered through a 0.22 μm PTFE membrane and washed with anhydrous acetone to completely remove the residuals. After drying in vacuum at 50 °C for 24 h, 0.3 g of SWNTs-NCO was dispersed in 20 mL of anhydrous acetone under sonication for

(36) Che, J. F.; Xiao, Y. H.; Wang, X. *Surf. Coat. Technol.* **2007**, *201*, 4578.

30 min, and then an excess of EDA (about 10 mL) was added under stirring in a dry nitrogen atmosphere at 60 °C for 24 h. After filtering, washing, and drying, functionalized SWNTs containing amino group (SWNTs-G_0-NH_2) were obtained.

As shown in Scheme 2, the grafting reaction and propagation of dendritic PAMAM from the SWNT surface was accomplished by repeating two processes: (1) Michael addition of MA to peripheral amino groups and (2) amidation of terminal ester groups by EDA. Michael addition of MA to peripheral amino groups was carried out as follows. 0.40 g of SWNTs-G_0-NH_2 was dispersed in 20 mL of methanol and then added to 40 mL of methanol/MA solution (1:1) to react at 30 °C for 48 h. The resultant was filtered, washed, and dried, yielding functionalized SWNTs containing the "first generation" ester group (SWNTs-$G_{0.5}$-$COOCH_3$). The amidation of the terminal groups of SWNTs-$G_{0.5}$-$COOCH_3$ was carried out by the same procedure as discussed above, except using EDA instead of MA, to obtain functionalized SWNTs containing "first generation" amino groups (SWNTs-G_1-NH_2). The propagation to higher generations was carried out by repeating Michael addition of MA to amino groups and amidation of terminal ester groups with EDA.

Spinning. Composite fibers with aligned SWNTs were prepared by solution blending followed by gelation spinning. Dendrimer-functionalized SWNTs at successive grafting generations from 0 to 2 were dispersed in acetonitrile (2 mg/mL) by 5 min/60 W sonication using a high-power cup-horn ultrasonic processor (Vibra-Cell, Sonics), followed by 2 h sonication in an ultrasonicator bath (S30H Elmasonic, Elma). Then Rutapox L20 resin was added to the suspensions. The mixture was magnetically stirred for 10 min, sonicated in a sonicator bath for 1 h, and vacuum degassed at 85 °C for 1 h to remove the solvent. The SL hardener (35 wt % of resin) was subsequently added to the solvent-free SWNT/L20 blend and mixed mechanically. Air bubbles were removed by vacuum pumping. Finally, composites containing 0.5 wt % of dendrimer-functionalized SWNTs at successive grafting generations from 0 to 2 were made up. The weight percent was in terms of the CNT weight, not the total filler weight.

Composite resins (and a control unreinforced resin) were loaded into a custom-built piston-type spinning device and maintained at 60 °C for about 50 min until they had reached their respective gel points (GPs), after which the spinning experiments were immediately carried out. The spinning apparatus consisted of a stainless steel barrel (3/4 in. i.d.) terminated by a Swagelok cap with a single spinneret hole of 1 mm diameter. The tube was heated with heating tape controlled at spinning temperature (60 °C) and pressurized by an actuator to extrude gelled resin at a rate of 80 mL/h. The extruded polymer fiber was air-cooled and drawn under tension by a windup spool located 20−40 cm from the spinneret. The windup speed was up to 300 rev/min with a mandrel having outer diameter of 70 mm. The fibers were cured at 60 °C for 4 h, 130 °C for 3 h, and then 180 °C for 12 h. As a second control, unreinforced epoxy resin was cast in a mold and cured under the same conditions.

Characterization. Infrared spectra for identification of the chemical groups on the SWNTs at various stages were recorded with a PE Paragon 1000 FTIR spectrometer from 400 to 4000 cm^{-1}. The weights of the samples and KBr were about 5 mg and 0.5 g, respectively. The pastes were pressed with 500 MPa. The ^1H NMR spectrum of functionalized SWNTs suspended in DMSO-d_6 was measured with a Bruker 500 MHz spectrometer. Thermogravimetric analysis (TGA) was performed with a Netzsch STA 409 PG/PC instrument at a heating rate of 20 °C /min from 50 to 800 °C in N_2 atmosphere.

Rheological measurements of the SWNTs-G_2-NH_2/EP (EP = epoxy) composite were performed on a Haake Rheostress 600 rheometer. The gel point (i.e., gelation time) was determined from the point of crossover of the shear storage (G') and loss (G'') moduli in small-amplitude oscillatory shear experiments at 60 °C. The rheometer was used in the parallel-plate configuration (diameter D = 25 mm, gap H = 1.0 mm) at a constant frequency of 1 Hz.

Scanning electron microscopy (SEM) measurements were carried out using a JEOL JSM-6700F field-emission scanning electron microscope (FE-SEM). The samples were lightly etched by reactive ion etching (RIE) using argon as the reactive gas to expose SWNTs on the surface of composite fibers, exploiting the different plasma stabilities of nanotubes and polymer. The etching was performed using a March PX-500 Cleaning System at 50 W and 10 sccm volumetric flow rate. Samples were etched for 10, 30, and 120 s.

Transmission electron microscopy (TEM) measurements were carried out on a JEOL 2010 scanning electron microscope, operated at 200 kV.

The distribution of nanotubes in the epoxy matrix was visually observed and photographed using a digital camera (Axiovert 200M, Zeiss) at 200× magnification.

An Instron model 5543 was used to perform tensile tests on single fibers, following the mounting specification indicated by ASTM standard C1557-03. A 10 N load cell was used to test the samples in uniaxial tension. The gauge lengths were 25 mm and the crosshead speed used was 2.54 mm/min. To ensure data accuracy and repeatability, multiple repeat tests were performed and the average of a minimum of ten valid values was used for the mechanical property analysis.
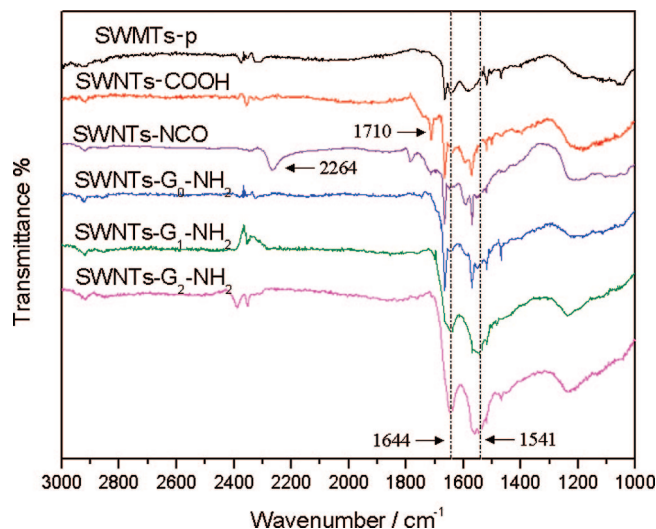
Results and Discussion

Dendrimer-Functionalization of SWNTs. As-received SWNTs-p have the form of tight networks of entangled, randomly oriented nanotube bundles (Figure 1a). After acid treatment, shortened, disentangled, straightened, small SWNT-COOH bundles of about 20 nm average diameter and several microns in length were obtained (Figure 1b). After the second-generation PAMAM functionalization, the SWNT bundles became smaller (ca. a few nanometers in diameter) and were covered with a sheath of the dendrimer (Figure 1c). As the sample was thoroughly washed to remove physically adsorbed dendrimer, this layer is interpreted to be grafted to the SWNTs.

The SWNT functionalization was characterized by FTIR (Figure 2). Compared with SWNTs-p, the spectrum of SWNTs-COOH exhibits a new absorption peak at 1710 cm^{-1} which is attributed to the C=O stretching modes of carboxyl groups on the SWNT surfaces generated by the mixed acid treatment. After reaction with excess TDI, the peak at 1710 cm^{-1} diminished while a significant increase of the NCO stretch at around 2264 cm^{-1} was observed. The reactivity of the isocyanate group at the para-position of TDI is higher than that at the ortho-position due to the steric hindrance of the methyl group. In the presence of excess TDI, there is preferential reaction of the *p*-isocyanate groups with SWNTs-COOH, resulting in a predominance of free *o*-isocyanate groups on the resulting SWNTs-NCO, which leads to the FTIR peak at 2264 cm^{-1}. The FTIR spectrum of SWNTs-G_0-NH_2 exhibits several changes from its precursors. First, the features at 2264 cm^{-1} (−NCO) and 1710 cm^{-1} (−COOH) are entirely absent, indicating complete reaction of the
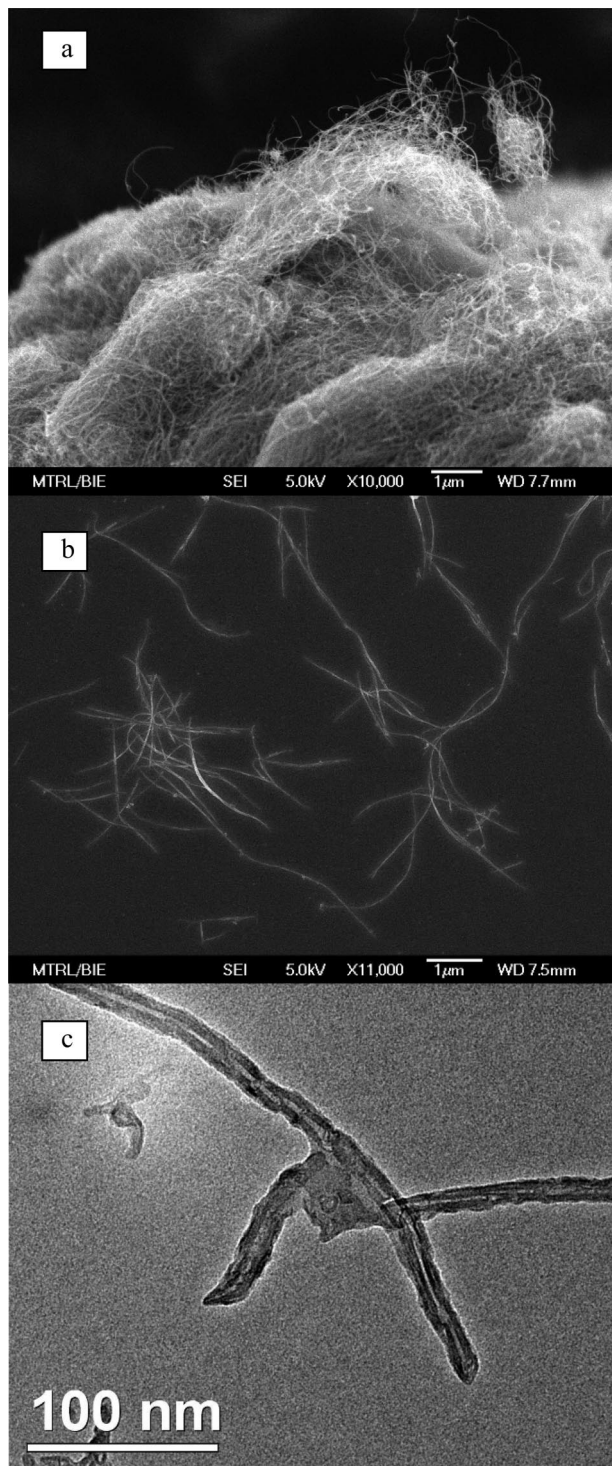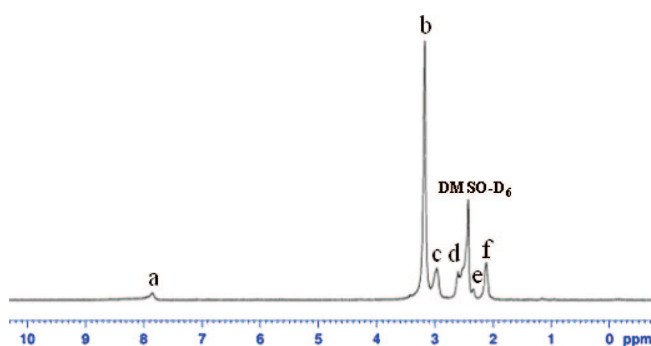
Figure 1. SEM images of SWNTs (a) before and (b) after acid treatment and (c) TEM image of SWNTs-G_2-NH_2.

Figure 2. FT-IR spectra of SWNTs at various stages of treatment/grafting.

Figure 3. ^{1}H NMR spectrum of SWNTs-G_2-NH_2 in DMSO-d_6.

isocyanate groups and the residual carboxyl groups in SWNTs-NCO. Second, new absorption features appear at 1644 and 1541 cm^{-1}; these are somewhat masked in the SWNTs-G_0-NH_2 spectrum by the complexity of the spectrum in the region 1500−1700 cm^{-1}, but their presence is evident in the substantial decrement in this region in comparison with that of the SWNT-NCO spectrum. The new features at 1644 and 1541 cm^{-1} are due to amide (−CO−NH−) I and II, indicating the introduction of amino groups onto the SWNTs-G_0-NH_2 surfaces through the grafting-from process. In the spectra of SWNTs-G_1-NH_2 and SWNTs-G_2-NH_2, the peaks

at 1644 and 1541 cm^{-1} are progressively stronger, indicating the presence of increasing amounts of PAMAM.

The structure of the dendrimer-modified SWNTs was further analyzed with NMR spectroscopy. Figure 3 shows the ^{1}H NMR spectrum of SWNTs-G_2-NH_2 samples, which have a high quantity of grafted dendrimer so that the polymer unit signals are very strong because of the excellent solubility of grafted SWNT. The hydrogen peaks of the grafted dendritic units (a, −CO−NH−; b, −NH−CH_2; c, −CH_2−NH_2; d, >N−CH_2; e, −CH_2−N<; and f, −CCO−CH_2−) are clearly detected in the ^{1}H NMR spectrum, confirming the chemical structure of the dendrimers.

The thermal properties of pristine and functionalized nanotubes were measured with TGA. Figure 4 shows that SWNTs-p lose about 0.75% of their initial weight when heated from 50 to 900 °C. The degradation onset temperature (T_{onset}) of SWNTs-COOH is 220 °C, decreasing to 150 °C for SWNTs-NCO, SWNTs-G_1-NH_2, and SWNTs-G_2-NH_2 due to the grafted organic and polymer molecules. The organic contents of the functionalized SWNTs-NCO, SWNTs-G_1-NH_2, and SWNTs-G_2-NH_2 estimated from the residual weight at 900 °C are 30%, 45%, and 60%, respectively.

Dendrimer-functionalized SWNTs are considerably more dispersible in epoxy than SWNTs-p. Figure 5 shows optical and SEM micrographs of composites with 0.5 wt % SWNTs content. SWNTs-p/EP composite has opaque SWNT agglomerations scattered throughout the matrix; the size of the
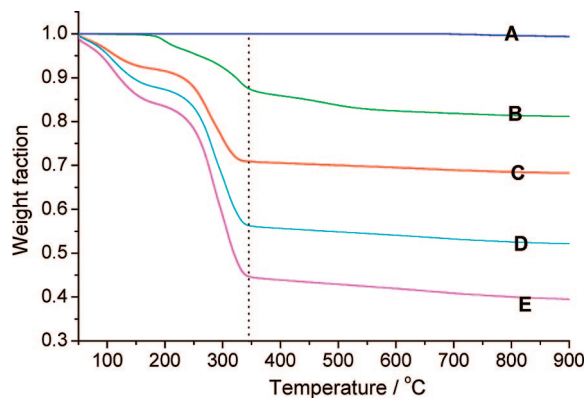
Figure 4. TGA curves of SWNTs-p (A), SWNTs-COOH (B), and functionalized nanotubes SWNTs-NCO (C), SWNTs-G_1-NH_2 (D), and SWNTs-G_2-NH_2 (E).
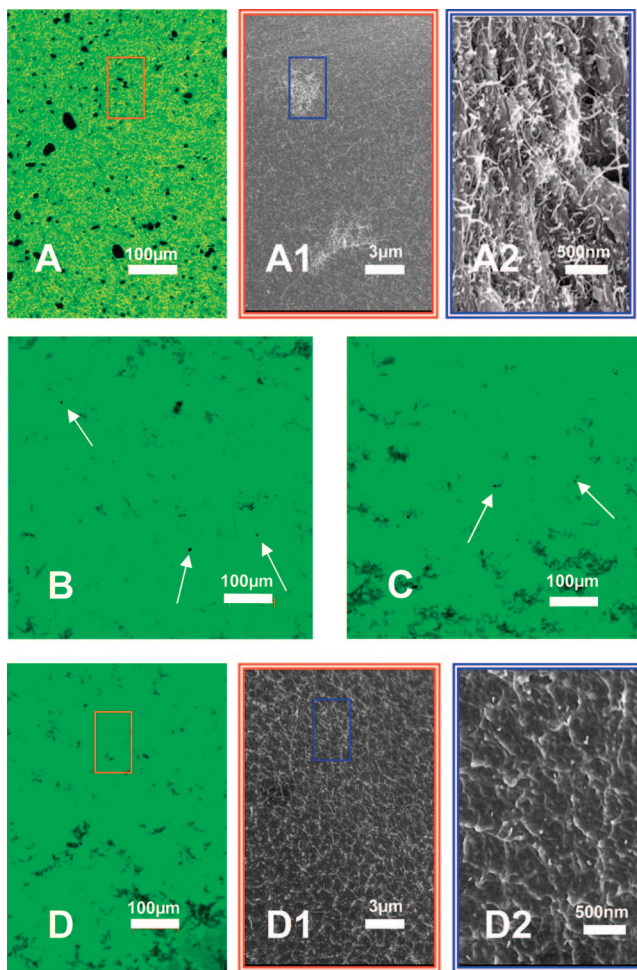
Figure 5. Microscopic image of SWNT/epoxy composites (0.5 wt %). Optical transmission micrographs of (A) SWNTs-p/EP, (B) SWNTs-G_0-NH_2/EP, (C) SWNTs-G1-NH_2/EP, and (D) SWNTs-G_2-NH_2/EP. A1, A2 and D1, D2 are progressive SEM enlargements of subregions in A and D, respectively. The enlarged regions are indicated by the colored outlines in A/A1 and D/D1.

larger agglomerations exceeds 10 μm (Figure 5A,A1,A2). The agglomerations have distinct edges and they have not integrated with the matrix. In the optical microscope images of SWNTs-G_0-NH_2/EP and SWNTs-G_1-NH_2/EP composites (Figure 5B,C), the nanotubes are dispersed much more uniformly and the agglomerations, much fewer in number, are tiny and loose (examples are highlighted by white arrows)
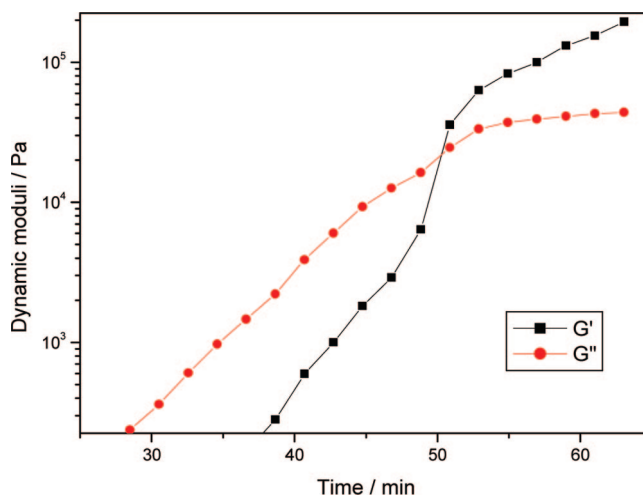

Figure 6. Time evolution of the storage (G') and loss (G'') moduli of reacting SWNTs-G_2-NH_2/EP system at 60 °C.

and have irregular and fuzzy edges. SWNTs-G_2-NH_2/EP composite appears to have the most uniform dispersion, with no visible agglomerations at 100× magnification (Figure 5D,D1,D2). Hence, the dispersibility of the nanotubes progressively increases with increasing dendrimer generation; Scheme 1 exhibits our proposed explanation for the trend. As the dendrimer generation increases, steric hindrance and hence debundling increase; also, the number of grafted amine functional groups and relative proportion of dendrimer increases so that the solubility and reactivity of the resulting higher generation dendritic PAMAM-functionalized CNTs increase.

Dendrimer-Functionalized SWNTs/EP Composite Fibers. Figure 6 shows the rheometry results for SWNTs-G_2-NH_2/EP composite determined at 60 °C. The curves of G' (shear storage modulus) and G'' (shear loss modulus) cross at 50 min, which is the gel point (GP).[37] Epoxy transforms from a liquid state to a gel state before finally reaching a solid state during curing. A cross-linking polymer at its GP is in a transition state between liquid and solid and has molecules with a broad range of molecular weights, ranging from small molecules to very large clusters. Also, at the GP the sample possesses elastic properties not present in the pregel state and the viscosity builds up rapidly. The resin system is spinnable while in the gel state. The optimum prespinning reaction condition for the SWNTs-G_2-NH_2/EP system was thus adopted to be 50 min at 60 °C.

Figure 7 shows optical micrographs of neat epoxy fiber and a series of composite fibers. The neat epoxy fiber has uniformly high transparency (Figure 7a). Fiber made of SWNT-p(0.5 wt %)/EP composite contains many opaque SWNT agglomerations with sizes up to more than 10 μm, scattered throughout a nearly transparent matrix (Figure 7b). In the SWNTs-G_2-NH_2/EP fibers (Figure 7c−e), the filler appears to be almost perfectly uniformly dispersed. No SWNT agglomeration is visible in these fibers. However, the fiber light transmission declines progressively with the addition of more CNTs; of the three formulations studied,

(37) Mortimer, S.; Ryan, A. J.; Stanford, J. L. *Macromolecules* **2001**, *34*, 2973.

Epoxy Fibers Reinforced with Single-Walled CNT

Chem. Mater., Vol. 21, No. 8, 2009 1477
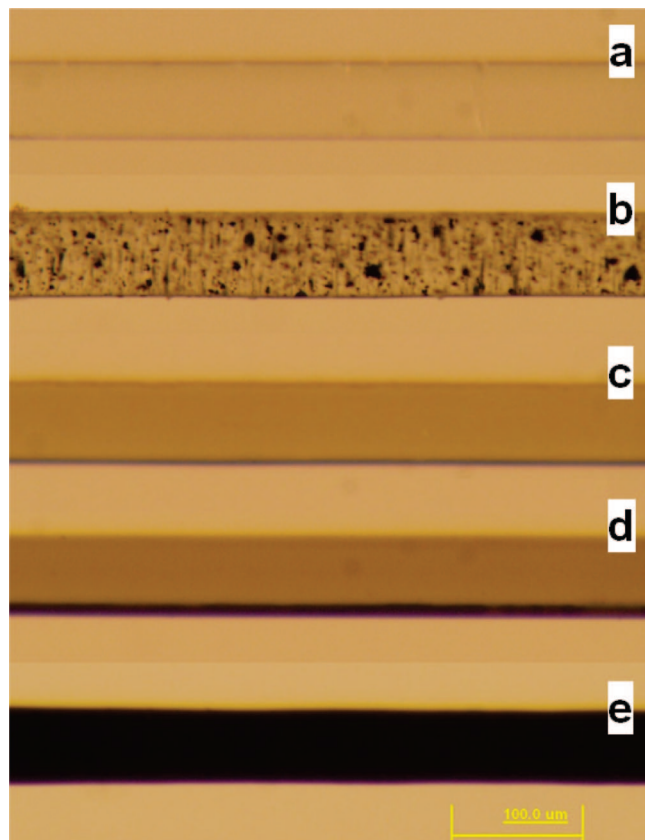
Figure 7. Optical micrographs of (a) neat EP fiber, (b) SWNTs-p/EP composite fiber, and SWNTs-G_2-NH_2/EP composite fibers with (c) 0.1 wt %, (d) 0.2 wt %, (e) 0.5 wt % SWNT filler.

only those with CNT content of 0.2% or less (Figure 7c,d) transmit significant light.

The SEM images in Figure 8 illustrate the β-alignment of well-dispersed SWNT-G_2-NH_2/EP in the composite fiber. In the cross-sectional image (Figure 8A), the axes of the SWNTs are all close to perpendicular to the cross section; not one nanotube lies horizontally across the cross section. There is also good uniformity of CNT dispersion in the matrix. The inset of Figure 8A shows a close-up of the cross section; the nanotubes are integrated with the polymer matrix and have broken rather than pulled out of the matrix. Some of the SWNT bundles seem to have partially pulled out before breaking; these are still clad with polymer matrix—the "halos" in Figure 8A are more than twice the diameter of the PAMAM sheath (Figure 1c)—which suggests that the SWNT/polymer bond is not weaker than the shear strength of the polymer, a highly desirable property in a filler. There manifestly is strong interfacial bonding between the epoxy matrix and the functionalized nanotubes, which aids efficient transfer of the stress load and prevents the sliding of nanotubes within the matrix under tension. A possible explanation for this is that the dendrimer promotes SWNT dispersion in the epoxy resin and the peripheral amino groups can bond covalently with the epoxy matrix.

To facilitate SEM imaging of nanotube longitudinal orientation, argon plasma etching was used to selectively etch away polymer matrix to expose SWNTs within the composite fibers; "as-spun" composite fibers have few SWNTs visible on the fiber surface, since they are well-aligned with the fiber
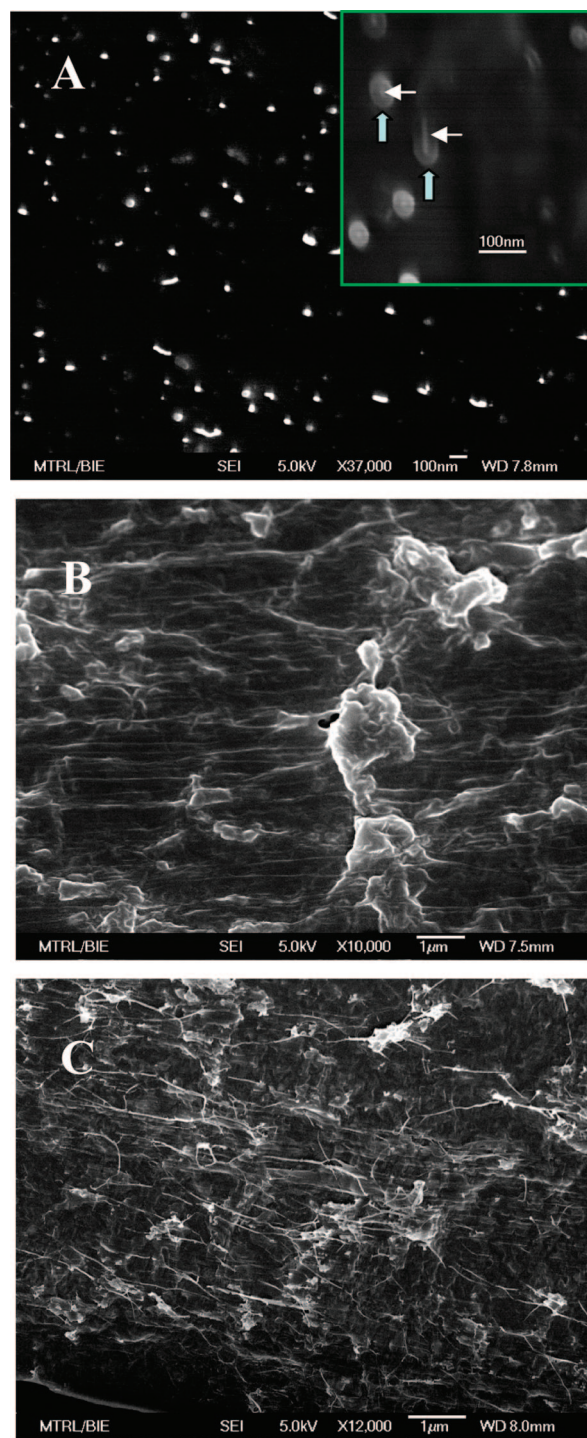
Figure 8. FESEM images of SWNT-G_2-NH_2/EP composite fibers (0.5 wt %): (A) cross section, (A inset) magnified cross section showing SWNT bundles (horizontal arrows) and adherent matrix (vertical arrows), and longitudinal view of fiber surface after argon plasma etching for (B) 10 s and (C) 30 s.

axis. Parts B and C of Figure 8 show composite fiber surfaces after, respectively, 10 s and 30 s plasma etching at 50 W with 10 sccm argon flow. Well-aligned longitudinally oriented SWNTs embedded within the polymer matrix become apparent with increased etching time. A much longer etch (120 s, data not shown) was found to significantly damage both the polymer matrix and the embedded nanotubes. These images demonstrate the excellent alignment of

Table 2. Yield Strength and Young's Modulus of Epoxy Casting and Epoxy Fibers

material	strength			Young's modulus		
	σ (MPa)	% increase compared to EP casting	% increase compared to pure EP fiber	E (GPa)	% increase compared to EP casting	% increase compared to pure EP fiber
EP casting	71.1 ± 2.9	–	–	1.75 ± 0.11	–	–
pure EP fiber	90.0 ± 5.0	26.6	–	3.30 ± 0.14	88.6	–
SWNTs-p/EP fiber	104.2 ± 4.1	46.6	15.8	3.47 ± 0.10	98.3	5.2
SWNTs-G_0-NH_2/EP fiber	117.0 ± 3.8	64.6	30.0	3.66 ± 0.12	109.1	10.9
SWNTs-G_1-NH_2/EP fiber	122.4 ± 2.5	72.2	36.0	3.72 ± 0.09	112.6	12.7
SWNTs-G_2-NH_2/EP fiber	125.1 ± 3.4	76.0	39.0	3.89 ± 0.17	122.3	17.9

SWNTs within the epoxy matrix that is produced by the spinning/drawing process.

Table 2 compares the measured Young's moduli and yield strengths of cast epoxy, unreinforced epoxy fibers, and composite fibers with SWNT-p filler as well as dendrimerized SWNT filler at successive grafting generations from 0 to 2. The SWNT contents are 0.5 wt %. Figure 9 shows their typical tensile stress−strain curves. The spun epoxy fibers have improved tensile properties compared with epoxy resin casting. The SWNTs-p have modest effect on the modulus and yield strength compared to the unreinforced epoxy spun fiber. The yield strength and moduli of composite fibers with dendrimer-functionalized SWNTs are significantly improved and increase progressively with generation number. Reinforcement of fibers with grafted-from SWNTs (i.e., SWNTs-G_{0-2}-NH_2) increases their yield strength by an average of 64.6%, 72.2%, and 76.0% above that of unreinforced epoxy casting and 30.0%, 36.0%, and 39.0% above that of spun pure epoxy fiber. The composite fibers also show significant improvement in Young's modulus: 109.1%, 112.6%, and 122.3%, respectively, for generations G_0, G_1, and G_2 compared to epoxy casting, and 10.9%, 12.7%, and 17.9% for G_0, G_1, and G_2 compared to spun pure epoxy fiber. The higher generation dendrimers manifestly do a better job of increasing fiber strength and modulus. The unreinforced epoxy fiber is somewhat stiffer and stronger than cast epoxy; this is due to reorientation of the epoxy resin network during the spinning/drawing process.

The amount of CNTs added in our composite is small, 0.5 wt %. Coleman et al. have used the rate of variation of
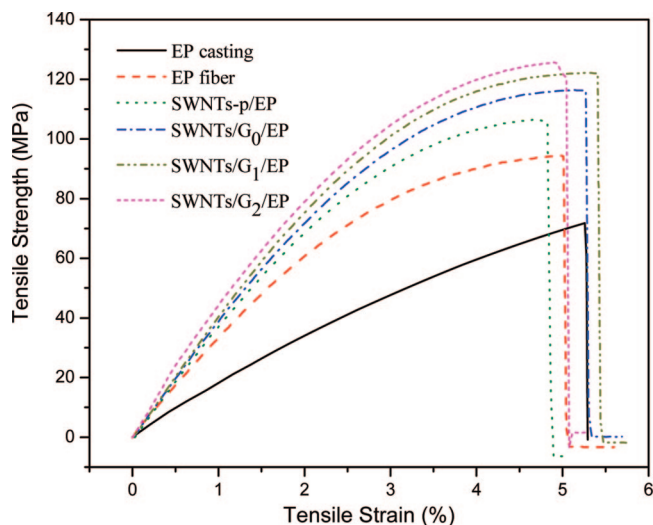
Figure 9. Typical tensile stress−strain curves of neat epoxy casting, epoxy fibers, and dendrimer-functionalized SWNTs/EP composite fibers at successive grafting generations from 0 to 2.

Young's modulus (E) with the volume fraction of CNTs (dE/dV_{NT}) as a yardstick to compare the reinforcement efficacy of CNTs in different modification methods.[1,38] Since there has been no report on the mechanical properties of aligned nanotube epoxy composite, the results of our study are compared to the data of randomly dispersed SWNT/epoxy composites that have been reported recently. Because most mechanical properties have been reported in terms of weight rather than volume fraction, the rate of variation of tensile strength and Young's moduli with weight fraction ($d\sigma/dW_{NT}$ and dE/dW_{NT}) are compared here (Table 1). In Table 1, we present comparison of our experimental results with annual averages from the literature of the reported reinforcement efficacy for SWNT-reinforced epoxy. For our aligned dendrimer-functionalized SWNTs-reinforced epoxy composite, the $d\sigma/dW_{NT}$ value is 7022 MPa and dE/dW_{NT} value is 118.0 GPa, which compares very favorably with the results reported in the recent literature. We attribute our high mechanical properties enhancement to two mechanisms: (i) The grafted-from PAMAM dendrimer acts as both a dispersing agent and a covalent matrix binding agent and (ii) alignment of the nanotubes along the fiber direction maximizes the effect of the filler on fiber tensile strength. The dendrimer solubility in the epoxy resin helps the nanotubes disperse in the matrix precursor. The dendrimer peripheral amino groups can react with epoxy groups, which improves stress transfer between CNTs and the epoxy resin and integration of CNTs into the cross-linked matrix. The progressive improvement in properties with dendrimer generation is presumably due to the increased debundling and number of reactive −NH_2 groups and consequent improved dispersion in and reaction with the matrix. Processing of CNTs into composite fibers with the CNTs aligned along the fiber axis is an effective way of manipulating the anisotropic properties of CNTs. This in turn permits the design of materials and products to take full advantage of the excellent axial tensile properties of SWNTs.

We used our reactive spinning to fabricate a laminate of unidirectional SWNT reinforced epoxy (Figure 10). To make this laminate, the collecting mandrel was translated in the longitudinal direction as the fibers were spinning. After spinning, the fiber belt was soaked in the mixture of L20 resin (75%) and SL hardener (25%), precured at 60 °C for 0.5 h, and then packed into a vacuum bag to get rid of air bubbles and remove excessive resin. The laminate was cured under the following conditions: 4 h at 60 °C, 3 h at 130 °C, and 12 h at 180 °C. Although further investigations are needed, the unidirectional laminate with aligned SWNTs is expected to be an advanced composite material possessing

(38) Coleman, J. N.; Khan, U.; Blau, W. J.; et al. *Carbon* **2006**, *44*, 1624.

Epoxy Fibers Reinforced with Single-Walled CNT

Chem. Mater., Vol. 21, No. 8, 2009 1479

Figure 10. Unidirectional SWNT-reinforced epoxy laminate made using a translating mandrel and reactive spinning.

high strength and light weight. The processing conditions have not been optimized for this laminate, and the mechanical data will be reported in the future.

Conclusion

We have demonstrated a practical method involving grafting PAMAM dendrimer from SWNTs and reactive spinning of SWNTs-G_n-NH$_2$/EP for achieving improved unidirectionally reinforced epoxy composite fibers. Reinforcement of fibers with aligned SWNTs-G_2-NH$_2$ (SWNT content 0.5 wt %) increases their yield strength and Young's modulus by an average of 76.0% and 122.3%, respectively, compared to unreinforced epoxy casting and 39.0% and 17.9%, respectively, compared to spun epoxy fiber. The SWNTs-G_2-NH$_2$/EP nanocomposite fibers possess a dσ/dW_{NT} value of 7022 MPa and a dE/dW_{NT} value of 118.0 GPa, which compare very favorably with results reported in the recent literature. The higher generation dendrimers manifestly do a better job of transferring stress from the matrix to the SWNTs. We attribute our high mechanical properties enhancement to two mechanisms: (i) the grafted-from PAMAM dendrimer acts both as a dispersing agent and a covalent matrix binding agent for efficient stress transfer from matrix to nanotubes and (ii) longitudinal alignment of the nanotubes along the fiber direction maximizes the reinforcement effect of the filler. Dendrimer-functionalized SWNTs are dramatically more dispersible in epoxy matrix than pristine SWNTs, and the dispersion of functionalized SWNTs improves with dendrimer generation number. Fibers reinforced with well-integrated and unidirectionally oriented SWNTs exploit the high and highly anisotropic tensile strength of nanotubes.